Gyrokinetic δf simulation of the collisionless and semicollisional tearing mode instability

W. Wan, Y. Chen, and S. E. Parker
University of Colorado, Boulder, Colorado 80309

(Received 18 August 2004; accepted 6 October 2004; published online 14 December 2004)

The evolution of collisionless and semicollisional tearing mode instabilities is studied using an electromagnetic gyrokinetic δf particle-in-cell simulation model. Drift-kinetic electrons are used. Linear eigenmode analysis is presented for the case of fixed ions and there is excellent agreement with simulation. A double peaked eigenmode structure is seen indicative of a positive Δ'. Nonlinear evolution of a magnetic island is studied and the results compare well with existing theory in terms of saturation level and electron bounce oscillations. Electron-ion collisions are included to study the semicollisional regime. The algebraic growth stage is observed and compares favorably with theory. Nonlinear saturation following the algebraic stage is observed. © *2005 American Institute of Physics*. [DOI: 10.1063/1.1827216]

I. INTRODUCTION

Tearing mode instabilities play an important roll in tokamak discharges. The basic process is the antiparallel magnetic field lines break and reconnect in the plasma to form magnetic islands. The perturbed vector potential is symmetric with respect to the central layer. The tearing mode instability can be described by the tearing mode parameter Δ', first introduced by Furth *et al.*,[1] where $\Delta'>0$ means unstable and $\Delta'<0$ means damping. Recently there have been many studies on other stabilizing and destabilizing mechanisms that affect the tearing. Especially for $\Delta'<0$, where an extra instability drive is needed to counteract the damping caused by negative Δ'. These mechanisms include destabilizing effects such as the bootstrap current for high pressure plasma which leads to neoclassical tearing mode,[2,3] and drift effects-(see, for example, Ref. 4) which are mainly stabilizing and lead to the drift tearing mode[5] especially in the case of small magnetic islands.

This paper focuses on simulation of the classical tearing mode instability caused by positive Δ'. Originally the instability was studied using resistive magnetohydrodynamics (MHD) theories,[1,6–14] in which resistivity is essential in the central layer, however, the outer regions are assumed nonresistive. The linear growth rate is then dependent on Δ' and resistivity. Hazeltine *et al.*[15] applied kinetic theory with collision operators and unified the previous MHD calculations. Later, Drake and Lee[16,17] extended the kinetic tearing mode theory to the collisionless regime, and thus the problem is divided into three regimes: collisionless, where the linear growth rate is much larger than collision frequency, i.e., $\gamma \gg \nu_c$; semicollisional regime where $\gamma \sim \nu_c$ and collisional where ν_c is large. The kinetic point of view of the basic physical process is that a perturbed current is produced by the induced electric field around the central layer, and this current drives tearing mode instability, thereby causing magnetic reconnection.

Kinetic simulations of collisionless tearing mode was first carried out by Katanuma and Kamimura[18] with a full kinetic particle code. Sydora[19] does the simulation using gyrokinetic-Vlasov equation, and applied realistic mass ratio ($m_i/m_e=1837$) and long time scale runs. Recently, Ricci *et al.*[20] studied the simulation of magnetic reconnection with an implicit particle-in-cell code in the limit of weakly magnetized plasma.

Our approach is to use a recently developed gyrokinetic δf particle-in-cell code[21,22] to study the tearing mode. Using the δf method allows accurate linear behavior and very clean nonlinear saturation. This simulation can use realistic physical parameters and can be pushed to box sizes a few hundreds ρ_i in the radial direction. The δf method is used to keep noise low. The fully nonlinear gyrokinetic equation for ions and drift kinetic equation for electrons are solved. We restrict our study to two dimensions by setting $k_z=0$.

Another result here is a pitch-angle scattering collision operator in the electron drift kinetic equation is used to study the tearing mode instability in the semicollisional regime. In this regime the nonlinear evolution of the tearing mode has three stages: early linear growth; then as the exponential growth slows down there is a stage in which the width of the magnetic island grows algebraically with time;[7,17] and the nonlinear saturation.[9,13,14] Our simulation results clearly show the algebraic growth stage, as well as the following final nonlinear saturation.

II. SIMULATION MODEL

A. The current profile

The physical current profile is similar to previous investigations.[18,19] We assume there is an equilibrium slab current in the z direction along a strong guiding field B_{z0}, with

$$J_{z0}(x) = -en_e u_0(x) = C_1 en_e e^{-(x-L_x/2)^2/a^2}. \quad (1)$$

a is the half-width and C_1 is the amplitude of the current, for which Refs. 18 and 19 have used the electron thermal velocity, i.e., $C_1=-v_{te}$, but any value can be used. For simplicity, we have set $T_i=T_e=m_e v_{te}^2$. An ion-electron mass ratio of 1837 is assumed throughout the paper.

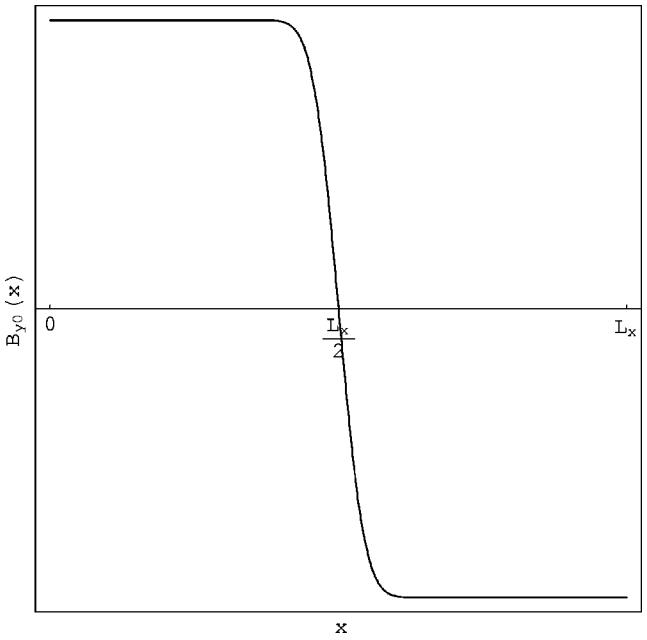

FIG. 1. The equilibrium antiparallel magnetic field in y direction.

In addition to the guiding field B_{z0}, the equilibrium current J_{z0} generates a field $B_{y0}(x)$ which has antiparallel field lines across $x=L_x/2$, shown in Fig. 1. The form of B_{y0} is

$$B_{y0}(x) = \frac{1}{2} e n_e C_1 \mu_0 a \sqrt{\pi}\, \mathrm{erf}\left(\frac{x - L_x/2}{a}\right), \tag{2}$$

where the erf(x) is the error function.

The perturbed magnetic field can be represented by a vector potential $\tilde{A}_z(x,y,t)$ through

$$\delta\mathbf{B} = \nabla \times (\tilde{A}_z \hat{z}) = \delta B_x \hat{\mathbf{x}} + \delta B_y \hat{\mathbf{y}}. \tag{3}$$

The boundary condition is periodic in the y and z directions and for x direction we have conducting wall boundary conditions:

$$\mathbf{A}(x) = \phi(x) = 0 \quad \text{for } x = 0 \text{ and } x = L_x. \tag{4}$$

There is no external electrostatic field and the total vector potential is $A_z = A_{z0} + \tilde{A}_z$, A_{z0} is induced by the equilibrium current that gives the B_{y0} field and satisfies the boundary condition $A_{z0}=0$ at $x=0$ and $x=L_x$. As mentioned earlier, we restrict our present study to two dimensions by keeping only the $k_z=0$ mode.

Since $B_{y0} \ll B_{z0}$, we can assume the parallel direction is the z direction and then the equilibrium electron distribution function is

$$F_0(x,\mathbf{V}) = \frac{1}{(2\pi)^{3/2} v_t^3} e^{-v_\perp^2/2v_t^2} \cdot e^{-[v_\parallel - u_0(x)]^2/2v_t^2}, \tag{5}$$

after integration over the perpendicular plane we have

$$f_0(x,v_\parallel) = 2\pi \int_0^\infty F_0(x,\mathbf{V}) v_\perp dv_\perp = \frac{1}{\sqrt{2\pi} v_t} e^{-[v_\parallel - u_0(x)]^2/2v_t^2}. \tag{6}$$

However, in the simulation code we use the canonical momentum $p_\parallel$ rather than $v_\parallel$ coordinate to eliminate difficulties with finite differencing $\partial A/\partial t$.[21] With $p_\parallel$ defined by

$$p_\parallel = v_\parallel + \frac{q}{m} \tilde{A}_z, \tag{7}$$

the actual zeroth-order distribution function for simulation is then

$$f_0(x,p_\parallel) = \frac{1}{\sqrt{2\pi} v_t} e^{-[p_\parallel - u_0(x)]^2/2v_t^2}. \tag{8}$$

B. Electron drift kinetic equation

We begin with the total electron distribution function

$$f_e = f_0(x,p_\parallel) + \delta f, \tag{9}$$

where $d\delta f(x,p_\parallel)/dt = -df_0(\mathbf{x},p_\parallel)/dt$. The electron drift-kinetic equation for δf is then

$$\frac{\partial \delta f}{\partial t} + \mathbf{V}_G \cdot \nabla\, \delta f + \dot{p}_\parallel \frac{\partial \delta f}{\partial p_\parallel} = -\left(v_\parallel \frac{\delta \mathbf{B}_\perp}{B_0} + \frac{\mathbf{E} \times \hat{\mathbf{b}}}{B_0}\right) \cdot \nabla f_0 - \dot{p}_\parallel \frac{\partial f_0}{\partial p_\parallel}. \tag{10}$$

The terms on the left-hand side can be evaluated by following particle trajectories, i.e., method of characteristics. $\mathbf{V}_G$ is the guiding center velocity,

$$\mathbf{V}_G \equiv v_\parallel \left(\hat{z} + \frac{B_{y0}}{B_0}\hat{y}\right) + v_\parallel \frac{\delta \mathbf{B}}{B_0} + \frac{\mathbf{E} \times \hat{\mathbf{b}}}{B_0}. \tag{11}$$

$\hat{\mathbf{b}}$ is the direction of magnetic field so that

$$\hat{\mathbf{b}} = \hat{\mathbf{z}} + \frac{B_{y0}}{B_0}\hat{\mathbf{y}}. \tag{12}$$

We should also note that in Eqs. (10) and (11) the $\hat{\mathbf{b}}$ and B_0 are only for the equilibrium magnetic field, the perturbed magnetic field is not included. The equation of motion for $\dot{p}_\parallel$ is

$$\begin{aligned} \dot{p}_\parallel &= \frac{dv_\parallel}{dt} + \frac{q}{m_e}\frac{\partial \tilde{A}_z}{\partial t} + \frac{q}{m_e}\mathbf{V}_G \cdot \nabla \tilde{A}_z \\ &= \frac{q}{m_e} E_\parallel + \frac{q}{m_e}\frac{\partial \tilde{A}_z}{\partial t} + \frac{q}{m_e}\mathbf{V}_G \cdot \nabla \tilde{A}_z \\ &= -\frac{q}{m_e}(\nabla \phi)_\parallel + \frac{q}{m_e}\mathbf{V}_G \cdot \nabla \tilde{A}_z. \end{aligned} \tag{13}$$

III. EIGENMODE ANALYSIS

Here, an eigenmode analysis of the collisionless linear tearing mode is given. According to Drake and Lee's theory,[16] in the collisionless and semicollisional limit, the perturbed electrostatic potential can be neglected, i.e., $\phi = \tilde{\phi} = 0$. The ion motion can be neglected as well since the half-width of the perturbed current Δ is much less than ρ_i. We will test this statement later in simulation but for now we accept $\tilde{\phi} = 0$ and eliminate ions response, then solve the linearized electron drift kinetic equation.

After linearizing Eq. (10), it becomes

$$\frac{\partial \delta f}{\partial t} + v_\parallel \frac{B_{y0}}{B_0}\frac{\partial \delta f}{\partial y} + v_\parallel \frac{\partial \delta f}{\partial z} = \left[- v_\parallel u_0'(x)\frac{\delta B_x}{B_0} + \dot{v}_\parallel \right] \frac{m_e[v_\parallel - u_0(x)]}{T_e} f_0(x, v_\parallel). \tag{14}$$

The $\mathbf{E}\times\mathbf{B}$ terms are neglected by assuming $\tilde{\phi} = 0$. We can then write the δB_x and and $\dot{v}_\parallel$ in terms of $\tilde{A}_z$ in Eq. (14),

$$\delta B_x = \frac{\partial}{\partial y}\tilde{A}_z \tag{15}$$

and

$$\dot{v}_\parallel = - \frac{e}{m_e}\tilde{E}_\parallel = \frac{e}{m_e}\frac{\partial}{\partial t}\tilde{A}_z. \tag{16}$$

Writing $\tilde{A}_z$ as $\tilde{A}_z(\mathbf{X}, t) = \tilde{A}_z(x) e^{i[(k_y y + k_z z) - \omega t]}$ and using

$$\frac{\partial}{\partial y} \to i k_y, \quad \frac{\partial}{\partial z} \to i k_z, \quad \frac{\partial}{\partial t} \to - i\omega, \tag{17}$$

Eq. (14) becomes

$$\delta f(x, v_\parallel) = \frac{1}{\omega - v_\parallel (k_z + B_{y0} k_y / B_0)} \left\{ \frac{e\omega}{T_e}[v_\parallel - u_0(x)] + \frac{m k_y}{T_e} v_\parallel [v_\parallel - u_0(x)] u_0'(x) \right\} f_0 \tilde{A}_z(x). \tag{18}$$

$\tilde{A}_z$ is induced by the perturbed current $\tilde{J}_z$ through the Ampère's law, and for the case that ions motion can be neglected the current is from electrons only:

$$\nabla_\perp^2 \tilde{A}_z = - \mu_0 \tilde{J}_z = \mu_0 n_0 e \int_{-\infty}^{\infty} dv_\parallel v_\parallel \delta f(x, v_\parallel). \tag{19}$$

With Eqs. (18) and (19), $k_z = 0$, a second-order ordinary differential equation is obtained for $\tilde{A}_z(x)$,

$$\frac{d^2}{dx^2}\tilde{A}_z(x) + q(x)\tilde{A}_z(x) = 0, \tag{20}$$

where

$$q(x) = - k_y^2 + \frac{\mu_0 n_0 e}{B_{y0} k_y T_e / B_0} \{ u_0(x)[e\omega + m k_y u_0'(x) u_0(x)] \langle V^1 \rangle + [e\omega + 2 m k_y u_0'(x) u_0(x)] \langle V^2 \rangle + m k_y u_0'(x) \langle V^3 \rangle \}. \tag{21}$$

We have defined $V \equiv v_\parallel - u_0(x)$ and the integrals

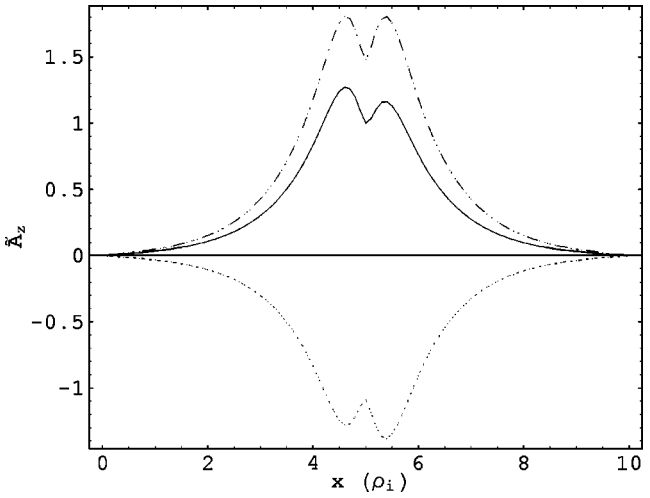

FIG. 2. $\tilde{A}_z(x)$ as the eigenfunction. Solid line, the real part, dotted line, the imaginary part, and dashed line, the absolute value. Plot is scaled to the unit that $\Re A_z(L_x/2) = 1$.

$$\langle V^n \rangle \equiv \frac{1}{\sqrt{2\pi} v_t} \int_{-\infty}^{\infty} dV \frac{V^n e^{-V^2/2v_t^2}}{V + u_0(x) - \omega B_0 / B_{y0} k_y} \tag{22}$$

can be integrated analytically.

We can numerically solve Eq. (20) as an eigenvalue problem for ω, using a shooting method, given $\tilde{A}(x) = 0$ at $x = 0$ and $x = L_x$. It turns out that for the physical parameters, ω is purely imaginary, therefore the linear growth rate is just $\gamma_k = \omega / i$.

The procedure here is very similar to that of Katanuma and Kamimura,[18] but in our result the eigenfunction of $\tilde{A}_z$ has a double peaked structure at the center, shown in Fig. 2, which is consistent with the fact that the tearing mode parameter,

$$\Delta' = \left[\frac{\partial}{\partial x}\tilde{A}_z\left(\frac{L_x}{2} + \lambda\right) - \frac{\partial}{\partial x}\tilde{A}_z\left(\frac{L_x}{2} - \lambda\right) \right] \Big/ \tilde{A}_z\left(\frac{L_x}{2}\right)$$

is positive, where λ is the width of the central layer. $\Delta' > 0$ is the condition of unstable tearing mode. For certain parameters Eq. (20) does not have an eigenvalue or eigenfunction, this corresponds to a stable system in simulation. The double peaked structure is observed for all the unstable tearing mode systems.

In Fig. 3 we compare the linear growth rate from small box simulations to the eigenmode result. This figure had been previously published in Ref. 22. We change $k_y a$ by changing a, the half-width of the equilibrium current, and $k_y = 2\pi / L_y$ is fixed. In both collisionless and collisional linear theories,[1,16,23] Δ' is determined by the two outer regions, which can be approximated as collisionless and $\Delta' a$ is a function of $k_y a$ only.

In Fig. 4 we plot the $\tilde{A}_z(x, y)$ from simulation at $y = L_y/2$, and compare to the real part of the eigenfunction $\tilde{A}_z(x)$. Both of them have the double peaked structure. Excellent agreement between the linear eigenmode theory and particle simulation is shown in Fig. 4.

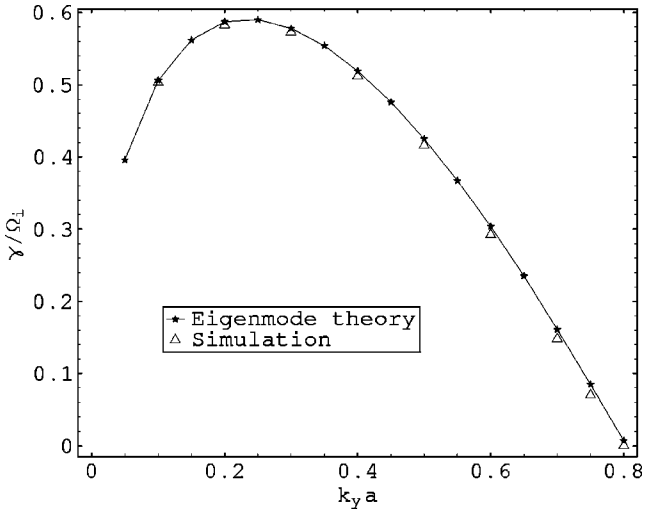

FIG. 3. Linear growth rate as a function of $k_y a$, compared to the eigenmode analysis. $L_x=2.5\rho_i$, $L_y=6.28\rho_i$, $\beta=0.1\%$, $C_1=-v_{te}$. a is varied and $k_y=1.0\rho_i^{-1}$ is fixed.

IV. SIMULATION RESULTS OF THE COLLISIONLESS TEARING MODE

A. Linear growth rate

According to the linear theories[16,18] derived from the electron drift kinetic equation, the collisionless linear growth rate is

$$\gamma_k = \frac{k_y v_{te} \Delta'}{2k_0^2 l_s}, \tag{23}$$

where v_{te} is the electron thermal velocity, $k_0^{-1}=c/\omega_{pe}$ and l_s is the magnetic shear length about $x=L_x/2$,

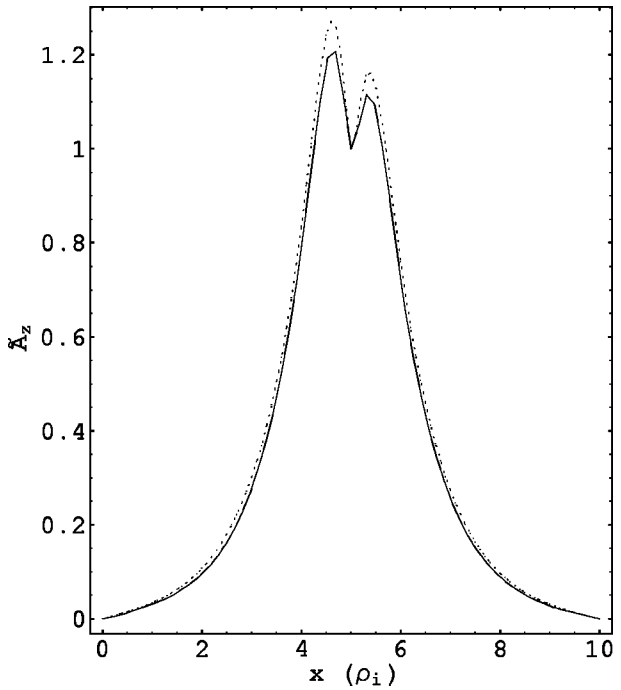

FIG. 4. Eigenfunction of $\tilde{A}_z(x)$, solid line is from simulation, and dotted line is from eigenmode calculation. $L_x=L_y=10\rho_i$, $\beta=1\%$, $a=0.5\rho_i$, and $C_1=-0.14v_{te}$.

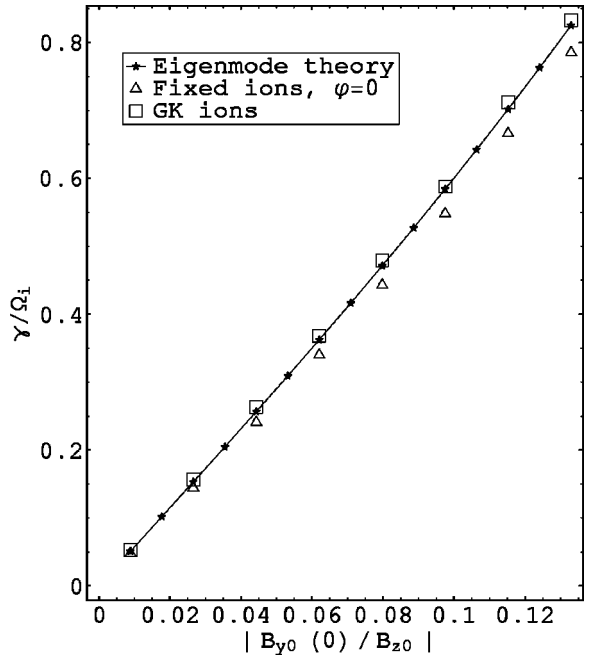

FIG. 5. Linear growth rate is proportional to amplitude of B_{y0}. $L_x=L_y=10\rho_i$, $a=0.5\rho_i$, and $\beta=1\%$. Amplitude of equilibrium current is varied to give different values of B_{y0}.

$$l_s \equiv \frac{B_{z0}}{\partial B_{y0}(x)/\partial x}. \tag{24}$$

Equations (23) and (24) make it clear that the collisionless linear growth rate is proportional to the amplitude of antiparallel magnetic field that induces the tearing mode instability, i.e., $\gamma_k \propto B_{y0}(0)/B_{z0}$. This result is observed in the eigenmode analysis and in simulation, shown in Fig. 5.

We see that for this $10\rho_i \times 10\rho_i$ box size, our simulation result with fixed ions and $\phi=0$ still agree with the eigenmode analysis, but not as well as for the $2.5\rho_i \times 6.28\rho_i$ small box simulation. This is due to the limit of grid points we have in x direction. In eigenmode analysis we have thousands of grid points in x but in simulation we have only 64, if we increase the number of grid points and number of particles we do have better agreement, but simulations become much more computationally demanding.

Simulation results with the full gyrokinetic ions response are also shown in Fig. 5. The growth rate is higher than for the case of fixed ions and $\phi=0$ simulation. This fact has also been found in Ref. 18 and is due to the electrostatic field ϕ. The $\mathbf{E}\times\mathbf{B}$ drift of electrons causes a perturbed current in the z direction $\tilde{J}_{zef}$ in addition to the $\tilde{J}_z$ caused by the induced electric field. Thus, the total perturbed current is increased and results in a higher growth rate.

For the results presented here, neglecting the ion response is reasonable for the small box simulations with $a=0.5\rho_i$. In such a case, with or without the ion response there is almost the same linear growth rate and nonlinear saturation level.

B. Nonlinear saturation level and the electron bounce frequency

Next, we discuss the nonlinear simulation results and how they compare with existing theory. Since $A_z(x,y) = A_{z0}(x,y) + \tilde{A}_z(x,y)$ is constant along a field line, the half-width of the magnetic island w is determined by $\tilde{A}_z$. In assuming that $\tilde{A}_z$ is constant across the central layer, i.e., $\tilde{A}_z(x,y) = \hat{A}_z \cos(k_y y)$, where $\hat{A}_z$ is the amplitude of the perturbed vector field, Refs. 23 and 17 show

$$w = 2\sqrt{\frac{\hat{A}_z l_s}{B_{z0}}}. \tag{25}$$

In Fig. 6, the time evolution of w is plotted using Eq. (25) as a solid line, where l_s is calculated using Eq. (24). The dotted line is a direct measure of w from the simulation, where we have used the fact that the "boundary" field line across the y axes is at the maximum and minimum value of $\tilde{A}(0,y)$. A square waveform appears in this diagnostic because we have only 32 grid cells in x.

As the island grows, eventually $w > \Delta_L$, and tearing mode instability enters the nonlinear phase. In this phase the tearing layer grows with the width of the island, thus the growth rate has to decrease so that the released magnetic energy can heat the larger number of particles inside the layer. Quantitatively, the saturation level of collisionless nonlinear tearing mode is predicted in Ref. 17 as

$$w = \frac{\Delta'}{2k_0^2 G}, \tag{26}$$

where $G = 0.410$ is a constant. To verify the nonlinear theory we combine Eq. (26) with Eq. (23) to get the relation of nonlinear saturation level and the linear growth rate

$$w = \frac{\gamma_k l_s}{k_y v_{te} G}. \tag{27}$$

We can calculate γ_k using eigenmode analysis and then use Eq. (27) to calculate the theoretical value of w at saturation level. For the case of Fig. 6 theoretical value of w is $0.597\rho_i$ and from simulation it is $0.585\rho_i$, so the nonlinear saturation level is well verified. Oscillations in Fig. 6 after saturation are due to the bounce motion of trapped electrons in the island, the frequency is[17]

$$\omega_b = k v_{te} w / 2 l_s. \tag{28}$$

Combining with Eq. (27) we obtain the following bounce frequency:

$$\omega_b = \gamma_k / 2G = 1.22\gamma_k. \tag{29}$$

From Fig. 6 the frequency is about $0.4\Omega_i$ and from Eq. (29) it is about $0.5\Omega_i$. Reference 18 also noted the fact that $\omega_b \approx \gamma_k$.

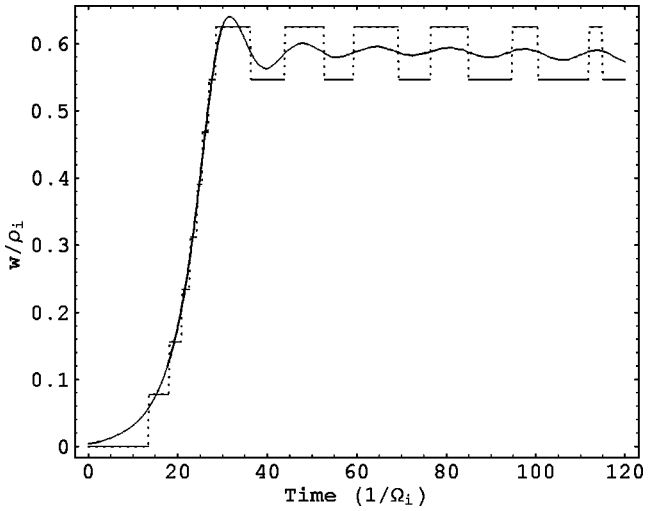

FIG. 6. Nonlinear evolution of the magnetic island width. Dotted line is measured directly from simulation and solid line is derived from the amplitude of $\tilde{A}_z$. $L_x = 2.5\rho_i$, $L_y = 6.28\rho_i$, $\beta = 0.1\%$, $a = 0.5\rho_i$, and $C_1 = -v_{te}$.

V. SIMULATION RESULTS OF THE SEMICOLLISIONAL TEARING MODE

In this section, initial studies of the semicollisional tearing mode are presented. We add a Lorentzian collision operator for electron-ion collisions to the electron drift kinetic equation (10):[21]

$$\frac{\partial f_e}{\partial t} + \mathbf{V}_G \cdot \boldsymbol{\nabla} f_e + \dot{p}_\parallel \frac{\partial f_e}{\partial p_\parallel} = C_L(f_e). \tag{30}$$

The operator is

$$C_L(f_e) = \nu_c \frac{1}{2}\frac{\partial}{\partial \lambda}\left[(1-\lambda^2)\frac{\partial}{\partial \lambda} f_e\right], \tag{31}$$

where $\lambda = v_\parallel / v$ is the pitch-angle parameter and ν_c the collision frequency. ν_c is generally dependent on v, but in our simulation ν_c is taken as a constant parameter, to be consistent with Ref. 17. The system is called "collisionless" when $\gamma_k \gg \nu_c$ and "semicollisional" when $\gamma_k \sim \nu_c$.

To determine the form of the collision operator, use $f_e = f_0 + \delta f$, so that

$$C_L(f_e) = C_L[f_0(x,p_\parallel)] + C_L(\delta f), \tag{32}$$

where f_0 is the the shifted Maxwellian distribution function (8). The second term is implemented using the Monte Carlo method.[21] In calculating $C_L[f_0(x,p_\parallel)]$ we only keep the term that is proportional to $\tilde{A}_z$, and the result is

$$C_L[f_0(x,p_\parallel)] = \frac{1}{2}\frac{e}{T}\tilde{A}_z \nu_c f_0(x,v_\parallel)\left\{\frac{u_0 m_e}{T}(v^2 - v_\parallel^2) - 2v_\parallel\left[1 + \frac{u_0 m_e}{T}(v_\parallel - u_0)\right] + \frac{u_0 m_e}{T}(v^2 - v_\parallel^2)\left[1 + \frac{u_0 m_e}{T}(v_\parallel - u_0)\right]\right\}. \tag{33}$$

For the $(v^2 - v_\parallel^2)$ terms in the Eq. (33), from $B\mu + m_e v_\parallel^2/2 = m_e v^2/2$ we have $v^2 - v_\parallel^2 = 2B\mu/m_e$.

The most significant character of collisional tearing mode is that there is an algebraic growth of the magnetic island in the nonlinear stage, as predicted theoretically by Rutherford[7] with MHD theory and by Drake and Lee[17] with kinetic theory. This algebraic growth stage has even been observed experimentally by Zhang *et al.*[24] for the evolution of the $m/n=2/1$ tearing mode in the Texas Experimental Tokamak.[25]

After the linear stage, the effective nonlinear growth rate becomes smaller, and when $\gamma < \nu_c$ the tearing mode enters the algebraic stage. Reference 17 predicts that

$$\gamma(t) = \frac{\nu_c \Delta'}{2k_0^2 G w(t)}. \tag{34}$$

Since $\gamma(t) = d \ln \hat{A}_z / dt$, Eq. (25) yields

$$\frac{dw}{dt} = \frac{\nu_c \Delta'}{4k_0^2 G}, \tag{35}$$

showing that the magnetic island width grows algebraically at this stage. Note this expression of dw/dt appears to be more accurate than the $dw/dt = \Delta' c^2/16G$ equation as in Ref. 17, since it indicates that dw/dt is proportional to ν_c and this is confirmed by the simulation results presented here. The tearing mode parameter Δ' is theoretically the same for both the collisionless and the semicollisional tearing mode, since it is determined by the two outer regions, which are taken to be collisionless. In deriving Eq. (34) Ref. 17 has used the linear Δ', which is a constant. For a more strict approach we should apply the nonlinear Δ' here, knowing the fact that the nonlinear Δ' decreases as the island width increases.[9,26] However, from the simulation results, we find that unlike Ref. 26, the nonlinear Δ' here does not decrease algebraically with the island width. In fact although it decreases much faster near the saturation and finally becomes negative, the nonlinear Δ' changes little during the algebraic growth stage, so in calculating Eq. (35) we can still use the linear Δ'.

To quantitatively compare Eq. (35) with simulation results, again, we need to rewrite it in terms of the collisionless linear growth rate γ_k, this is done by combining Eq. (35) with Eq. (23), to obtain

$$\frac{dw}{dt} = \frac{\nu_c \gamma_k l_s}{2G k_y v_{te}}. \tag{36}$$

Condition for the validity of Eq. (34) and hence Eq. (36) is

$$\Delta_{sc} \ll w \ll a, \tag{37}$$

where Δ_{sc} is the half-width of $\tilde{J}_z$ of the linear semicollisional tearing instability and is related to its collisionless counterpart as $\Delta_{sc} \approx \Delta_k (\nu_c/\gamma_k)^{2/3}$.[16] Since for the semicollisional tearing mode $\gamma_k \sim \nu_c$, to ensure Eq. (37) we need a small Δ_k ($\Delta_k \ll \rho_i$ is the condition for tearing mode to neglect ions response). According to the collisionless linear theory $\Delta_k \approx 1/k_0^2 a$, then Eq. (37) requires

$$1/k_0^2 \ll a^2. \tag{38}$$

Since $k_0^{-1} = c/\omega_{pe}$ and $[\rho_i/(c/\omega_{pe})]^2 = \beta m_i/m_e$, Eq. (38) becomes

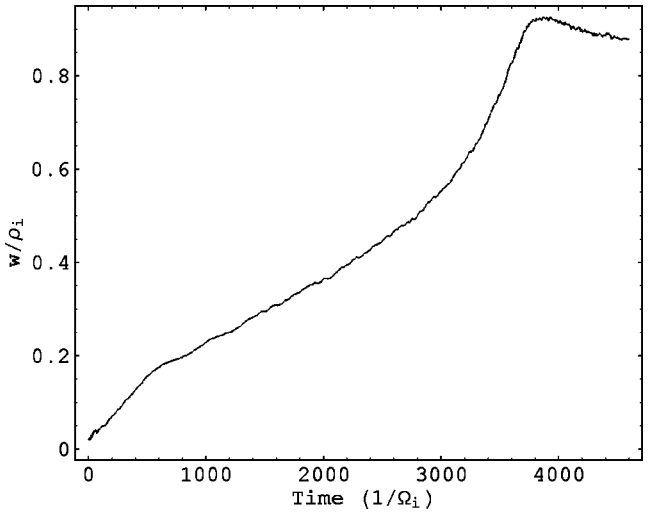

FIG. 7. Nonlinear evolution of semicollisional tearing mode. $L_x = 10\rho_i$, $L_y = 10.28\rho_i$, $a = \rho_i$, $\beta = 1\%$, and $C_1 = -0.02 v_{te}$. $\nu_c = 0.003\Omega_i$.

$$\beta \frac{m_i}{m_e} \gg \left(\frac{\rho_i}{a}\right)^2. \tag{39}$$

Because of this, our code is well suited to observe the algebraic growth stage in the semicollisional tearing mode. For simulations with L_x up to $10\rho_i$, a is generally smaller than or comparable with ρ_i, then Eq. (39) means $\beta m_i/m_e \gg 1$, and the so-called "high β" problem of gyrokinetic PIC simulation has just recently been solved and implemented in our code.[21]

In Fig. 7 we present results with a $10\rho_i \times 10.28\rho_i$ simulation of the nonlinear semicollisional tearing mode. $a = \rho_i$, $\beta = 1\%$. We have made the equilibrium current small so that the linear growth rate of the collisionless tearing mode from eigenmode analysis is $\gamma_k = 0.009\Omega_i$, which is comparable to $\nu_c = 0.003\Omega_i$. From about $t = 600\Omega_i^{-1}$ to $t = 2800\Omega_i^{-1}$ we see a clear algebraic growth stage. Linear fitting of this stage gives $dw/dt = 1.48 \times 10^{-4} \rho_i \Omega_i$. The theoretical value can be calculated using Eq. (36), the result is $dw/dt = 1.51 \times 10^{-4} \rho_i \Omega_i$, in good agreement with simulation.

The nonlinear saturation level of the collisionless tearing mode with these parameters is at $w = 0.14\rho_i$. Theoretically,[17] at this level $w \approx \Delta_k$ (in our model, $w = 2.4\Delta_k$ actually). Since $\Delta_k \approx \Delta_{sc} (\gamma_k/\nu_c)^{2/3}$, we can see from Fig. 7 the algebraic growth starts well after the collisionless saturation level, where $w \gg \Delta_{sc}$ is satisfied.

In Fig. 8, we show the dw/dt results with different collision frequencies ranged from $\nu_c = 0.0005\Omega_i$ to $\nu_c = 0.004\Omega_i$. The simulation results agree fairly well with theory for $0.0005 \leqslant \nu_c/\Omega_i \leqslant 0.003$, showing the proportional relation of dw/dt and ν_c. Simulations with larger collision rates are more demanding, since the size of the random change in the pitch-angle variable λ in a time step Δt is proportional to $\sqrt{\nu_c \Delta t}$. Smaller Δt has to be used for larger ν_c to approximate the diffusive process in pitch-angle scattering. The fact that for $\nu_c/\Omega_i \geqslant 0.004$ simulation results are less than Eq. (35) is not well understood at this time. It is plausible that for larger ν_c values the plasma enters the collisional regime, and the semicollisional kinetic theory begins to fail.

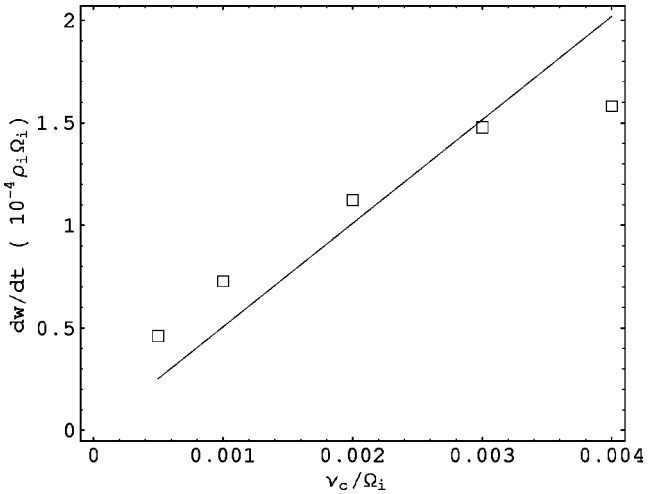

FIG. 8. dw/dt as a function of ν_c. Solid line represents theoretical values calculated using Eq. (36) and squares are from simulation.

After the algebraic growth stage we see the instability finally saturates at about $w=a$, which is much bigger than the collisionless saturation level. White *et al.*[9] first studied the saturation of nonlinear resistive tearing mode and it has also been observed in experiment.[24] In Fig. 9 we show simulation results of the saturation levels with different collision frequencies. Simulations at larger collisionality are difficult because as the saturation level increases $\delta f/f$ becomes large and the benefit of δf algorithm is lost, thereby requiring a much larger number of particles. Because of these numerical constrains we have limited our simulation time. However, particle number convergence has been tested. Also, the very weak collisionality regime is very important for many tokamak plasmas. Figure 9 indicates the saturation level is dependent on ν_c, and the higher ν_c, the higher saturation level. It is understandable that in the transition from the collisionless regime to collisional regime, for smaller collisional frequency the saturation level is smaller, because finally when

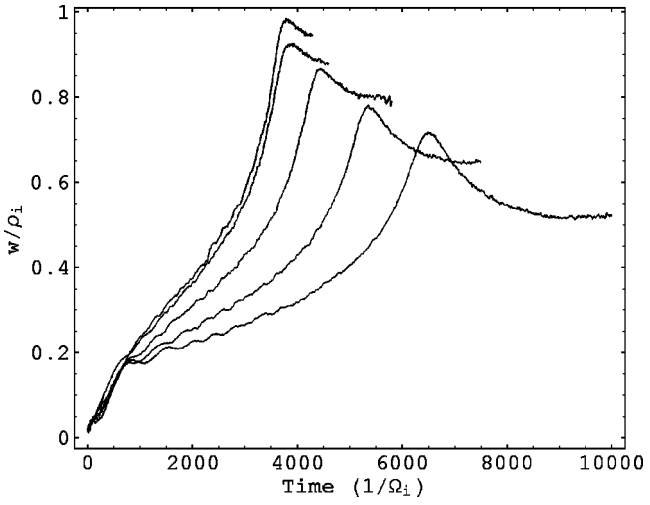

FIG. 9. Nonlinear evolution of the semicollisional tearing mode with different values of collision frequency. Same parameters as Fig. 8. ν_c equals to $0.0005\Omega_i$, $0.001\Omega_i$, $0.002\Omega_i$, $0.003\Omega_i$, and $0.004\Omega_i$ for saturation levels from low to high, respectively.

ν_c is zero, we have the collisionless saturation level, which is at $w=0.14\rho_i$, and much smaller than the saturation levels of semicollisional tearing mode presented here. Recent studies with reduced MHD theory[13,14] show that in the limit of small w compared to current width, the saturation level is proportional to Δ' and independent of resistivity. If these theories are applied the collisional saturation level should be at $w=1.22\Delta' a^2$, larger than the semicollisional saturation levels observed here. It is reasonable to expect that for larger ν_c's the saturation levels will converge. However, we note that in our simulation $a=\rho_i$ is small and at the saturation level w is comparable to a, thus the MHD theories cannot be applied.

VI. SUMMARY

The evolution of the collisionless and semicollisional tearing mode was studied using a recently developed δf particle-in-cell simulation model. Linear simulation results are benchmarked with eigenmode analysis for the case of fixed ions. A double humped eigenmode structure was observed in both the eigenmode analysis and simulation corresponding with positive Δ'. Simulation results compared favorably to theory in linear growth rate, nonlinear saturation level and electron bounce frequency. In simulations with a narrow current layer ($a\sim\rho_i$), we verified the assumption that the ions response can be neglected. The semicollisional tearing mode was studied by including electron-ion collisions and the nonlinear algebraic growth was observed in simulation for the first time. The algebraic growth rate scaling with collisionality agrees quantitatively with theory at small collisionality. Nonlinear saturation following the algebraic growth phase was observed. These are promising results and we plan to extend this work to three dimensions and larger island size in the near future.

ACKNOWLEDGMENTS

The authors thank Dan Barnes, Giovanni Lapenta, and Richard Sydora for helpful discussions.

This work was supported by the Department of Energy, Office of Fusion Energy Science.

[1] H. P. Furth, J. Killeen, and M. N. Rosenbluth, Phys. Fluids **6**, 459 (1963).
[2] (See National Technical Information Service Document No. DE86008946) W. X. Xu and J. D. Callen, University of Wisconsin Plasma Report No. UWPR 85-5, 1985. Copies may be ordered from the National Technical Information Service, Springfield, VA 22161.
[3] R. Carrera, R. D. Hazeltine, and M. Kotschenreuther, Phys. Fluids **29**, 899 (1986).
[4] Q. Yu, S. Günter, and B. D. Scott, Phys. Plasmas **10**, 797 (2003).
[5] P. H. Rutherford and H. P. Furth, Princeton PPPL, Report No. MATT-872, 1971 (unpublished).
[6] H. P. Furth, P. H. Rutherford, and H. Selberg, Phys. Fluids **16**, 1054 (1973).
[7] P. H. Rutherford, Phys. Fluids **16**, 1903 (1973).
[8] A. H. Glasser, J. M. Green, and J. L. Johnson, Phys. Fluids **18**, 875 (1975).
[9] R. B. White, D. A. Monticello, M. N. Rosenbluth, and B. V. Waddell, Phys. Fluids **20**, 800 (1977).
[10] M. Kotschenreuther, R. D. Hazeltine, and P. J. Morrison, Phys. Fluids **28**, 294 (1985).
[11] C. M. Bishop, J. W. Connor, R. J. Hastie, and S. C. Cowley, Plasma Phys. Controlled Fusion **33**, 389 (1991).
[12] D. Biskamp, *Nonlinear Magnetohydrodynamics* (Cambridge University Press, Cambridge, 1993).

[13]F. Militello and F. Porcelli, Phys. Plasmas **11**, L13 (2004).
[14]D. F. Escande and M. Ottaviani, Phys. Lett. A **323**, 278 (2004).
[15]R. D. Hazeltine, D. Dobrott, and T. S. Wang, Phys. Fluids **18**, 1778 (1975).
[16]J. F. Drake and Y. C. Lee, Phys. Fluids **20**, 1341 (1977).
[17]J. F. Drake and Y. C. Lee, Phys. Rev. Lett. **39**, 453 (1977).
[18]I. Katanuma and T. Kamimura, Phys. Fluids **23**, 2500 (1980).
[19]R. D. Sydora, Phys. Plasmas **8**, 1929 (2001).
[20]P. Ricci, J. U. Brackbill, W. Dauphton, and G. Lapenta, Phys. Plasmas **11**, 4102 (2004).
[21]Y. Chen and S. Parker, J. Comput. Phys. **189**, 463 (2003).
[22]S. E. Parker, Y. Chen, W. Wan, B. I. Cohen, and W. M. Nevins, Phys. Plasmas **11**, 2594 (2004).
[23]R. J. Goldston and P. H. Rutherford, *Introduction to Plasma Physics* (Institute of Physics, Bristol, 1995), pp. 337–361.
[24]Y. Z. Zhang, R. Denton, S. M. Mahajan, C. Jiayu, and A. Wootton, Phys. Rev. Lett. **65**, 2877 (1990).
[25]A. J. Wooton, B. A. Carreras, H. Matsumato, K. McGuire, W. A. Peebles, Ch. P. Ritz, P. W. Terry, and S. J. Zweben, Phys. Fluids B **2**, 2879 (1990).
[26]Q. Yu, S. Günter, and K. Lackner, Phys. Plasmas **11**, 140 (2004).